Shape-based approach for solar sail trajectory optimization

Andrea Caruso, Alessandro A. Quarta*, Giovanni Mengali

Dipartimento di Ingegneria Civile e Industriale, University of Pisa, Italy

Matteo Ceriotti

James Watt School of Engineering, University of Glasgow, Scotland, United Kingdom

Abstract

The analysis of the optimal control law that steers a solar sail-based spacecraft from a given initial condition toward a final target state is typically carried out using either indirect or direct approaches. Both these methods are usually time-consuming and require good initial guesses of costates or state vector. This paper presents a procedure requiring minimum user-computer interaction to compute an approximate three-dimensional optimal trajectory using a shape-based approach. To that end, novel shaping functions are introduced to describe the time evolution of the spacecraft state vector. The optimization problem is solved using a genetic algorithm, in which a set of shape coefficients and the initial and final spacecraft position are computed while enforcing suitable constraints on the magnitude and direction of the propulsive acceleration vector. Numerical simulations of transfers from Earth to potentially hazardous asteroids show that this method provides good estimates of solar sail trajectories, which can be used as guesses for more refined direct optimization approaches.

Keywords: solar sail, trajectory optimization, shape-based method

Nomenclature

$\boldsymbol{a}$	=	propulsive acceleration, [mm/s^2]
a	=	semimajor axis, [AU]
a_c	=	characteristic acceleration, [mm/s^2]
$a_{\max}$	=	maximum magnitude of propulsive acceleration, [mm/s^2]
a_r	=	radial component of $\boldsymbol{a}$, [mm/s^2]
a_t	=	transverse component of $\boldsymbol{a}$, [mm/s^2]
a_p,λ_p,ϕ_p	=	shape parameters of p
a_h,a_k,b_h,b_k,λ_{hk},ϕ_{hk}	=	shape parameters of h and k
e	=	eccentricity
f,g	=	in-plane equinoctial elements
h,k	=	out-of-plane equinoctial elements
i	=	inclination, [deg]
L	=	true longitude, [deg]
N	=	number of discretization arcs
n_{rev}	=	number of revolutions around the Sun
$\hat{\boldsymbol{n}}$	=	outward normal unit vector
p	=	semilatus rectum, [AU]

*Corresponding author

Email addresses: andrea.caruso@ing.unipi.it (Andrea Caruso), a.quarta@ing.unipi.it (Alessandro A. Quarta), g.mengali@ing.unipi.it (Giovanni Mengali), matteo.ceriotti@glasgow.ac.uk (Matteo Ceriotti)

Published in Aerospace Science and Technology, Vol. 107, December 2020, pp. 106363 (1–8). doi: https://doi.org/10.1016/j.ast.2020.106363

r	=	Sun-spacecraft distance, [AU]
$\boldsymbol{r}$	=	position vector, [AU]
$\hat{\boldsymbol{r}}$	=	radial unit vector
r_x,r_y,r_z	=	components of $\boldsymbol{r}$ in Cartesian coordinates, [AU]
$r_\oplus$	=	reference distance, 1 AU
s	=	success rate
T	=	flight time, [TU]
t	=	time, [TU]
Δ	=	dimensionless error in the flight time
ϵ,ϵ_t	=	tolerance value
λ_{fg},ϕ_{fg}	=	shape parameters of f and g
$\mu_\odot$	=	Sun's gravitational parameter, [$\mathrm{AU}^3/\mathrm{TU}^2$]
ν	=	true anomaly, [deg]
$\boldsymbol{\xi}$	=	state vector
Ω	=	right ascension of the ascending node, [deg]
ω	=	argument of pericenter, [deg]

Subscripts

0	=	initial time
f	=	final time
ind	=	refers to indirect method
MS	=	refers to multiple-shooting method
SB	=	refers to shape-based method

Superscripts

$\cdot$	=	time derivative

1. Introduction

Solar sailing is an innovative and fascinating form of propulsion that requires no propellant consumption to produce thrust, which, instead, is generated exploiting the solar radiation pressure [1]. Due to its propellantless nature, a solar sail-based spacecraft can be used to perform advanced space missions that would be difficult to carry out with traditional chemical thrusters, such as maintenance of artificial equilibrium points [2, 3], generation of (non-Keplerian) displaced orbits [4], and asteroid tour [5, 6].

Optimization of solar sail trajectories is usually carried out using either indirect or direct approaches [7]. Indirect methods use the analytical necessary conditions from the calculus of variation and Pontryagin's maximum principle to formulate a two-point boundary value problem, whose solution gives the optimal control law capable of transferring the spacecraft from a given initial condition toward a final target state [8]. This approach has the advantage that the optimal control law can be usually determined analytically [9, 10], but the nonlinearity of the problem induces a high sensitivity to the initial guess of costates. Direct methods, instead, transcribe a continuous optimal control problem into a nonlinear programming problem by partitioning in time the state vector and the control law. The latter are usually simpler to implement than the indirect ones, but give approximate optimal solutions only and require a good initial estimate to find optimal transfers [11].

To overcome the disadvantages of both the above approaches, new methods have been developed, able to generate fast approximations of spacecraft trajectories for a preliminary evaluation of the required flight time or to be used as initial guesses for a direct approach. Shape-based methods describe a low-thrust trajectory with analytical expressions [12, 13, 14], which are functions of a suitable set of parameters. After having calculated the time derivative of the position vector, it is possible to retrieve the spacecraft velocity and acceleration, while the propulsive acceleration history is obtained by exploiting the equations of motion. Suitable constraints may be also enforced on the propulsive acceleration to get feasible trajectories. Other authors have also proposed to use finite Fourier series [15, 16] or Bézier curves [17, 18] to shape the spacecraft trajectory, or to use deep neural networks to estimate the transfer time [6]. The shape-based method has

also been proved to be effective in producing good initial guesses to more complex and refined optimization techniques [19].

Recently, methods for rapid generation of solar sail trajectories have been developed. An example is the shape-based approach introduced by Peloni et al. [5] for the design of multiple near-Earth-asteroid missions, in which the spacecraft state evolution, described using modified equinoctial elements, is expressed as a function of four design parameters. However, the approach described in [5] presents some limitations. First of all, it is valid for coplanar transfer scenarios only. Moreover, the constraint that relates the direction and magnitude of the propulsive acceleration is not considered in the optimization problem, so that the shaped trajectory can be different from that actually tracked by a solar sail. For this reason, the procedure of [5] uses the error between the final state obtained by numerical integration and the final desired state as its objective function.

The aim of this paper is to illustrate a procedure that generates an initial estimate of a solar sail trajectory by generalizing the method discussed in [5] to the case of three-dimensional transfer scenarios. Moreover, to avoid the need of numerical integrations, an analysis is carried out to identify a suitable set of constraints (which also take into account the relation between the sail attitude and the propulsive acceleration components) to obtain a trade-off solution between approximation accuracy and computational effort. The proposed method is validated considering both orbit-to-orbit and rendezvous transfer heliocentric scenarios. The introduction of new shape functions and of constraint equations that model the physics of solar sails allows better estimate of sail trajectories to be obtained when compared to previous shape-based methodologies existing in the literature. Notably, the proposed approach requires a minimum user-computer interaction and, as such, it is more suited than either an indirect approach or the recent method by Caruso et al. [16] to deal with those cases when a large number of flight scenarios needs to be investigated.

2. Mathematical model

Consider a heliocentric orbit-to-orbit transfer of a solar sail-based spacecraft, in which the initial and final orbits are described by the Keplerian elements $\{a, e, i, \Omega, \omega\}$, where a is the semimajor axis, e is the eccentricity, i is the inclination, Ω is the right ascension of the ascending node, and ω is the argument of pericenter. Assuming a flat sail without degradation effects [20] and using an ideal force model [21], the sail propulsive acceleration vector is

$$\boldsymbol{a} = a_c \left(\frac{r_\oplus}{r}\right)^2 (\hat{\boldsymbol{n}} \cdot \hat{\boldsymbol{r}})^2 \, \hat{\boldsymbol{n}} \tag{1}$$

where r is the Sun-spacecraft distance, $\hat{\boldsymbol{r}}$ is the Sun-spacecraft unit vector, $\hat{\boldsymbol{n}}$ is the unit vector normal to the sail surface in the direction opposite to the Sun, and a_c is the characteristic acceleration, defined as the propulsive acceleration magnitude produced by a Sun-facing sail (i.e. when $\hat{\boldsymbol{n}} \equiv \hat{\boldsymbol{r}}$) at a reference distance $r_\oplus \triangleq 1\,\mathrm{AU}$. The value of a_c is assumed as a constant of motion, because in this work the uncertainties due to solar irradiance fluctuations [22] are neglected. The time variation of $\boldsymbol{a}$ is usually obtained as the solution of an optimal control problem, in which the solar sail-based spacecraft heliocentric equation of motion is

$$\ddot{\boldsymbol{r}} = -\frac{\mu_\odot}{r^3}\boldsymbol{r} + \boldsymbol{a} \tag{2}$$

where $\mu_\odot$ is the Sun's gravitational parameter, and $\boldsymbol{r} = r\,\hat{\boldsymbol{r}}$ is the spacecraft position vector. The next section describes a procedure able to generate a rapid estimate of the time-variation of the propulsive acceleration vector in an assigned (heliocentric) mission scenario using a shape-based approach.

2.1. Trajectory shape functions

Assume that the sail state is described using modified equinoctial elements [23, 24], that is, the state vector is $\boldsymbol{\xi} \triangleq [p, f, g, h, k, L]^{\mathrm{T}}$, with

$$p = a(1 - e^2) \tag{3}$$
$$f = e\cos(\Omega + \omega) \tag{4}$$
$$g = e\sin(\Omega + \omega) \tag{5}$$
$$h = \tan(i/2)\cos(\Omega) \tag{6}$$
$$k = \tan(i/2)\sin(\Omega) \tag{7}$$
$$L = \Omega + \omega + \nu \tag{8}$$

where ν is the true anomaly, and L is the true longitude. The variation of the modified equinoctial elements $\{p, f, g, h, k\}$ with the true longitude L is modelled through the following shape functions that extend the expressions proposed in [5] to a three-dimensional mission scenario

$$p(L) = \tilde{p}_0 + \tilde{p}_f(L - L_0) + a_p(L - L_0)^2 + \lambda_p \sin(L - L_0 + \phi_p) \tag{9}$$
$$f(L) = \tilde{f}_0 + \tilde{f}_f(L - L_0) + \lambda_{fg} \sin(L - L_0 + \phi_{fg}) \tag{10}$$
$$g(L) = \tilde{g}_0 + \tilde{g}_f(L - L_0) - \lambda_{fg} \cos(L - L_0 + \phi_{fg}) \tag{11}$$
$$h(L) = \tilde{h}_0 + \tilde{h}_f(L - L_0) + a_h \exp[b_h(L - L_0)] + \lambda_{hk} \sin[2(L - L_0) + \phi_{hk}] \tag{12}$$
$$k(L) = \tilde{k}_0 + \tilde{k}_f(L - L_0) + a_k \exp[b_k(L - L_0)] - \lambda_{hk} \cos[2(L - L_0) + \phi_{hk}] \tag{13}$$

where L_0 is the value of the true longitude at the initial time t_0, while a_p, λ_p, ϕ_p, λ_{fg}, ϕ_{fg}, a_h, b_h, a_k, b_k, λ_{hk}, ϕ_{hk}, $\tilde{p}_0$, $\tilde{p}_f$, $\tilde{f}_0$, $\tilde{f}_f$, $\tilde{g}_0$, $\tilde{g}_f$, $\tilde{h}_0$, $\tilde{h}_f$, $\tilde{k}_0$, and $\tilde{k}_f$ are design parameters. The capability of Eqs. (9)–(13) to describe an orbit-to-orbit (optimal) heliocentric transfer trajectory has been investigated in a number of test cases. In particular, classical interplanetary transfers (toward Mars, Venus, and Mercury), and transfers toward a set of near Earth asteroids (of which the orbital elements are listed in Table 1) have been analyzed. Recall that there exist more than 22000 known near Earth asteroids, each one with peculiar orbital characteristics. To reduce such a huge amount of possible scenarios, this study deals with transfers toward near Earth asteroids with $i < 20\,\mathrm{deg}$ and $e < 0.4$ only. The four celestial bodies in Table 1 have been considered to represent different possible scenarios toward orbits with high or low values of inclination and eccentricity. Moreover, two values of characteristic acceleration have been considered, that is, $a_c = \{0.2, 0.6\}\,\mathrm{mm/s^2}$, which are representative of low- or high-performance solar sails, respectively.

Celestial body	a (AU)	e	i (deg)	Ω (deg)	ω (deg)
2011 CG2	1.177	0.1586	2.76	293.23	283.85
2009 CQ5	0.9328	0.0915	18.68	278.69	118.2
1992 FE	0.9287	0.406	4.71	311.93	82.61
1620 Geographos	1.245	0.3354	13.34	337.2	276.92

Table 1: List of target asteroids and their orbital elements.

In each test case, a reference (optimal) orbit-to-orbit transfer trajectory has been obtained with an indirect approach by adapting the procedure described in [8]. Note that, in this study, the indirect method has been used to obtain the reference trajectory in a few test cases only. In fact, solving an optimal control problem using an indirect approach usually requires a complex (and time-consuming) procedure to guess the initial values of the adjoint variables [7, 25]. However, in the initial phase of mission design, when a large number of transfer scenarios has to be analyzed (consider, for example, a multiple-asteroid mission [6]), minimum user-computer interaction is desired to automate the whole procedure, so that an indirect method-based procedure is typically unsuitable.

Using the results of an indirect optimization, in terms of L-variation of the modified equinoctial elements $\{p, f, g, h, k\}$, the value of each design parameter in Eqs. (9)–(13) has been determined through a fitting

procedure with a nonlinear least square method, using the MATLAB Curve Fitting toolbox. The quality of the fit is reassumed in Table 2, in terms of sum of squares due to error (SSE) and coefficient of determination (R-square). In particular, the closer the value of SSE (or R-square) to zero (or one), the better the analytical expressions of Eqs. (9)–(13) fit the results obtained through an indirect approach.

Target orbit	a_c (mm/s^2)	p	f	g	h	k
2011 CG2	0.2	$6 \times 10^{-4}/0.991$	$1.7 \times 10^{-3}/0.964$	$6 \times 10^{-4}/0.989$	$8 \times 10^{-6}/0.976$	$2 \times 10^{-5}/0.985$
2011 CG2	0.6	$1 \times 10^{-6}/1$	$8 \times 10^{-6}/0.999$	$1 \times 10^{-5}/0.999$	$9 \times 10^{-6}/0.985$	$2 \times 10^{-5}/0.996$
2009 CQ5	0.2	$3 \times 10^{-4}/0.997$	$2.8 \times 10^{-3}/0.854$	$9 \times 10^{-4}/0.884$	$5 \times 10^{-6}/0.998$	$1 \times 10^{-4}/0.999$
2009 CQ5	0.6	$3.5 \times 10^{-3}/0.989$	$0.1058/0.522$	$0.024/0.727$	$6 \times 10^{-5}/0.987$	$3 \times 10^{-4}/0.998$
1992 FE	0.2	$5 \times 10^{-4}/0.996$	$1.8 \times 10^{-3}/0.995$	$1.6 \times 10^{-3}/0.99$	$9 \times 10^{-6}/0.995$	$3 \times 10^{-6}/0.999$
1992 FE	0.6	$1.5 \times 10^{-3}/0.996$	$3.7 \times 10^{-3}/0.99$	$1 \times 10^{-2}/0.976$	$3 \times 10^{-5}/0.991$	$4 \times 10^{-6}/0.999$
Geographos	0.2	$1 \times 10^{-3}/0.987$	$1.6 \times 10^{-3}/0.931$	$2.5 \times 10^{-3}/0.992$	$7 \times 10^{-5}/0.998$	$7 \times 10^{-5}/0.988$
Geographos	0.6	$1.9 \times 10^{-3}/0.983$	$2.3 \times 10^{-3}/0.979$	$5.3 \times 10^{-3}/0.99$	$4 \times 10^{-4}/0.995$	$3.7 \times 10^{-4}/0.977$
Mars	0.2	$7 \times 10^{-4}/0.999$	$1.6 \times 10^{-3}/0.956$	$1.7 \times 10^{-3}/0.904$	$3 \times 10^{-6}/0.99$	$6 \times 10^{-6}/0.983$
Mars	0.6	$4 \times 10^{-6}/1$	$1 \times 10^{-5}/1$	$7 \times 10^{-6}/1$	$9 \times 10^{-6}/0.986$	$1 \times 10^{-5}/0.976$
Venus	0.2	$2 \times 10^{-5}/0.999$	$9 \times 10^{-6}/0.999$	$3 \times 10^{-5}/0.998$	$4 \times 10^{-7}/0.997$	$8 \times 10^{-6}/0.998$
Venus	0.6	$4 \times 10^{-5}/0.999$	$2 \times 10^{-5}/0.999$	$1 \times 10^{-5}/0.999$	$2 \times 10^{-5}/0.979$	$1 \times 10^{-4}/0.98$
Mercury	0.2	$1 \times 10^{-4}/0.999$	$3 \times 10^{-4}/0.979$	$5.6 \times 10^{-3}/0.907$	$9 \times 10^{-6}/0.998$	$1 \times 10^{-5}/0.998$
Mercury	0.6	$3 \times 10^{-4}/0.999$	$6 \times 10^{-4}/0.998$	$0.022/0.899$	$4 \times 10^{-5}/0.994$	$1 \times 10^{-4}/0.987$

Table 2: Statistical values of fit (SSE/R-square).

The values in Table 2 are consistent with the results of [5], which have been obtained in a two-dimensional scenario. Accordingly, the shape functions given by Eqs. (9)–(13) are used in the procedure described in the next section, which allows the optimal (three-dimensional) solar sail transfer trajectory to be obtained using a shape-based approach.

2.2. Trajectory optimization using shape-based method

The optimization of the sail transfer trajectory consists in evaluating the subset of design parameters a_p, λ_p, ϕ_p, λ_{fg}, ϕ_{fg}, a_h, b_h, a_k, b_k, λ_{hk}, ϕ_{hk}, and the initial and final true longitude, L_0 and L_f, that minimize the flight time T given by [13]

$$T = \int_{L_0}^{L_f} \frac{\mathrm{d}t}{\mathrm{d}L} \mathrm{d}L \simeq \int_{L_0}^{L_f} \frac{1}{\sqrt{\mu_\odot p}} \left(\frac{p}{1 + f\cos L + g\sin L} \right)^2 \mathrm{d}L \tag{14}$$

with the constraints

$$\max_t(\|\boldsymbol{a}\| - a_{\max}) < 0 \tag{15}$$

$$\min_t(a_r) > 0 \tag{16}$$

$$\max_t(|a_r - a_c\big(r_\oplus/r\big)^2(\hat{\boldsymbol{n}} \cdot \hat{\boldsymbol{r}})^3|) < \epsilon \tag{17}$$

$$\max_t(|a_t - a_c\big(r_\oplus/r\big)^2(\hat{\boldsymbol{n}} \cdot \hat{\boldsymbol{r}})^2 \ \|\hat{\boldsymbol{r}} \times \hat{\boldsymbol{n}}\| \ |) < \epsilon \tag{18}$$

where $a_{\max} = a_c(r_\oplus/r)^2$ is the maximum magnitude of the propulsive acceleration at a distance r from the Sun, a_r (or a_t) are the components of $\boldsymbol{a}$ along the radial (or transverse) direction, and ϵ is a given (small) tolerance value. Note that Eqs. (17)-(18) are not considered in [5], and their introduction allows a more accurate approximation of a feasible solar sail trajectory to be obtained. In Eqs. (15)–(18), an expression of $\boldsymbol{a}$ as a function of the modified equinoctial elements can be obtained from Eq. (2) by adapting the procedure described in [13]. To that end, the cartesian components of the sail position vector $\boldsymbol{r} = [r_x, r_y, r_z]^{\mathrm{T}}$ are

written as

$$r_x = \frac{p[\cos L + (h^2 - k^2)\cos L + 2hk \sin L]}{(1 + f\cos L + g\sin L)(1 + h^2 + k^2)} \tag{19}$$

$$r_y = \frac{p[\sin L - (h^2 - k^2)\sin L + 2hk \cos L]}{(1 + f\cos L + g\sin L)(1 + h^2 + k^2)} \tag{20}$$

$$r_z = \frac{2p[h\sin L - k\cos L]}{(1 + f\cos L + g\sin L)(1 + h^2 + k^2)} \tag{21}$$

The first and the second derivatives of $\boldsymbol{r}$ are then obtained as

$$\dot{\boldsymbol{r}} = \frac{\mathrm{d}\boldsymbol{r}}{\mathrm{d}L}\frac{\mathrm{d}L}{\mathrm{d}t} \tag{22}$$

$$\ddot{\boldsymbol{r}} = \frac{\mathrm{d}\dot{\boldsymbol{r}}}{\mathrm{d}L}\frac{\mathrm{d}L}{\mathrm{d}t} \tag{23}$$

with

$$\frac{\mathrm{d}L}{\mathrm{d}t} \simeq \sqrt{\mu_\odot p}\left(\frac{1 + f\cos L + g\sin L}{p}\right)^2 \tag{24}$$

and

$$\frac{\mathrm{d}\boldsymbol{r}}{\mathrm{d}L} = \frac{\partial \boldsymbol{r}}{\partial p}\frac{\partial p}{\partial L} + \frac{\partial \boldsymbol{r}}{\partial f}\frac{\partial f}{\partial L} + \frac{\partial \boldsymbol{r}}{\partial g}\frac{\partial g}{\partial L} + \frac{\partial \boldsymbol{r}}{\partial h}\frac{\partial h}{\partial L} + \frac{\partial \boldsymbol{r}}{\partial k}\frac{\partial k}{\partial L} + \frac{\partial \boldsymbol{r}}{\partial L} \tag{25}$$

$$\frac{\mathrm{d}\dot{\boldsymbol{r}}}{\mathrm{d}L} = \frac{\partial \dot{\boldsymbol{r}}}{\partial p}\frac{\partial p}{\partial L} + \frac{\partial \dot{\boldsymbol{r}}}{\partial f}\frac{\partial f}{\partial L} + \frac{\partial \dot{\boldsymbol{r}}}{\partial g}\frac{\partial g}{\partial L} + \frac{\partial \dot{\boldsymbol{r}}}{\partial h}\frac{\partial h}{\partial L} + \frac{\partial \dot{\boldsymbol{r}}}{\partial k}\frac{\partial k}{\partial L} + \frac{\partial \dot{\boldsymbol{r}}}{\partial L} \tag{26}$$

where

$$\frac{\partial p}{\partial L} = \tilde{p}_f + 2a_p(L - L_0) + \lambda_p \cos(L - L_0 + \phi_p) \tag{27}$$

$$\frac{\partial f}{\partial L} = \tilde{f}_f + \lambda_{fg}\cos(L - L_0 + \phi_{fg}) \tag{28}$$

$$\frac{\partial g}{\partial L} = \tilde{g}_f + \lambda_{fg}\sin(L - L_0 + \phi_{fg}) \tag{29}$$

$$\frac{\partial h}{\partial L} = \tilde{h}_f + a_h b_h \exp[b_h(L - L_0)] + 2\lambda_{hk}\cos[2(L - L_0) + \phi_{hk}] \tag{30}$$

$$\frac{\partial k}{\partial L} = \tilde{k}_f + a_k b_k \exp[b_k(L - L_0)] + 2\lambda_{hk}\sin[2(L - L_0) + \phi_{hk}] \tag{31}$$

Finally, the values of the (remaining) coefficients $\tilde{p}_0$, $\tilde{p}_f$, $\tilde{f}_0$, $\tilde{f}_f$, $\tilde{g}_0$, $\tilde{g}_f$, $\tilde{h}_0$, $\tilde{h}_f$, $\tilde{k}_0$, and $\tilde{k}_f$ are obtained by enforcing the initial and final conditions on the position and velocity vectors [13].

The optimization problem is solved using the Augmented Lagrangian Genetic Algorithm [26, 27, 28] implemented in MATLAB. The output of the genetic algorithm is further refined using a local optimizer based on the built-in function *fmincon*. In the optimization process, a population size of 20 individuals has been used for the genetic algorithm, whereas *fmincon* uses an active-set algorithm with a maximum number of function evaluation equal to 3000; other options are set to their default values. A scaled problem is considered in the numerical simulations, so that a unit of length is defined as 1 AU, and the Sun's gravitational parameter is $\mu_\odot = 1$. As a result, a unit of time is TU $\simeq 58.13$ days.

3. Numerical Simulations

The shape-based procedure described in the preceding section is now applied to some sample mission scenarios to generate solar sail feasible transfer trajectories. In particular, three different approaches are compared: 1) a method that uses the shape functions (9)–(13) and considers the constraints (15)-(18) in the optimization process; 2) a simplified method that uses the shape functions (9)–(13) with constraints (15)-(16) only; 3) a method that uses the linear-trigonometric shape functions defined in [13] and considers only a constraint on the maximum value of the propulsive acceleration magnitude.

The method 2 is considered to assess the effect of the constraint equations (17)-(18) on the generation of a good guess of a solar sail trajectory. Indeed, an approach that only takes into account Eqs. (15)-(16) is able to significantly decrease the required computational time, as will be shown in the succeeding discussion. The third method, instead, is analyzed to make a comparison with an approach that (similarly to this manuscript) describes the spacecraft state vector using a set of analytical expressions for the modified equinoctial elements, but does not include any constraint on the sail propulsive acceleration.

Two transfer scenarios are analyzed departing from the Earth's orbit toward those of potentially hazardous asteroids. Such asteroids have been thoroughly observed and studied because of their high collision probability with the Earth [29] and to characterize their physical and dynamical properties in order to choose a suitable strategy to deflect or destroy the small celestial body. For this reason, the recent literature [5, 6] has also proposed them as candidate targets of space missions. In particular, the asteroids 2002 DU3 [30] and 2007 MK13 [31] have been considered in this manuscript to quantify the performance of the shape-based method in the case of a transfer toward target orbits with non-negligible final eccentricity or high inclination; see Table 3. In these examples, a solar sail with $a_c = 0.3\,\mathrm{mm/s^2}$ has been considered, and the bounds of the shape parameters defined in Eqs. (9)–(13) are specified in Table 4.

celestial body	a (AU)	e	i (deg)	Ω (deg)	ω (deg)
Earth	1	0.0167	0	0	102.94
2002 DU3	1.145	0.2382	8.7	0.69	245.53
2007 MK13	1.025	0.1398	19.88	95.09	259.96

Table 3: Orbital parameters of Earth, asteroid 2002 DU3 and asteroid 2007 MK13.

Parameter	lower bound	upper bound
λ_p	0	0.1
λ_{fg}	0	0.3
λ_{hk}	0	0.1
$\phi_p, \phi_{fg}, \phi_{hk}$	0	2π
a_p	0	0.01
a_h, b_h	-0.3	0.3
a_k, b_k	-0.3	0.3

Table 4: Lower and upper bounds for the design parameters.

For each transfer scenario, methods 1–3 have been executed 100 times, and a success rate s_{SB} has been computed, which corresponds to the number of times the shape-based method is able to converge towards a feasible optimal solution. Then, all the 100 solutions of methods 1–3 (even the unfeasible ones) have been used as initial guesses for a direct method, and a success rate s_{MS} has been computed. To that end, a direct multiple-shooting technique [7] has been used, which partitions the whole trajectory into $N \in \mathbb{N}^+$ arcs of equal duration and $N+1$ nodes. The spacecraft state is propagated along each arc by numerical integration of the equation of motion (2) using a fourth order Runge-Kutta integration scheme. Boundary conditions and continuity of the states at the nodes are finally enforced to obtain a feasible solar sail trajectory. The resulting nonlinear programming problem is solved using CasADi software package [32] and IPOPT solver [33]. All the numerical simulations have been carried out on a personal computer with an Intel processor Core i7-4770

CPU at 3.40 GHz and with 16 GB of RAM. Note that a number of discretization points equal to 100 has been considered for the direct multiple-shooting method.

In the case of method 1, the success rate is shown in Figs. 1(a) and 1(c) as a function of the tolerance value $\epsilon = \{10^{-3}, 5\times10^{-3}, 10^{-2}, 1.7\times10^{-2}, 5\times10^{-2}, 10^{-1}\}\,\mathrm{AU/TU^2}$; see Eqs. (17)-(18).

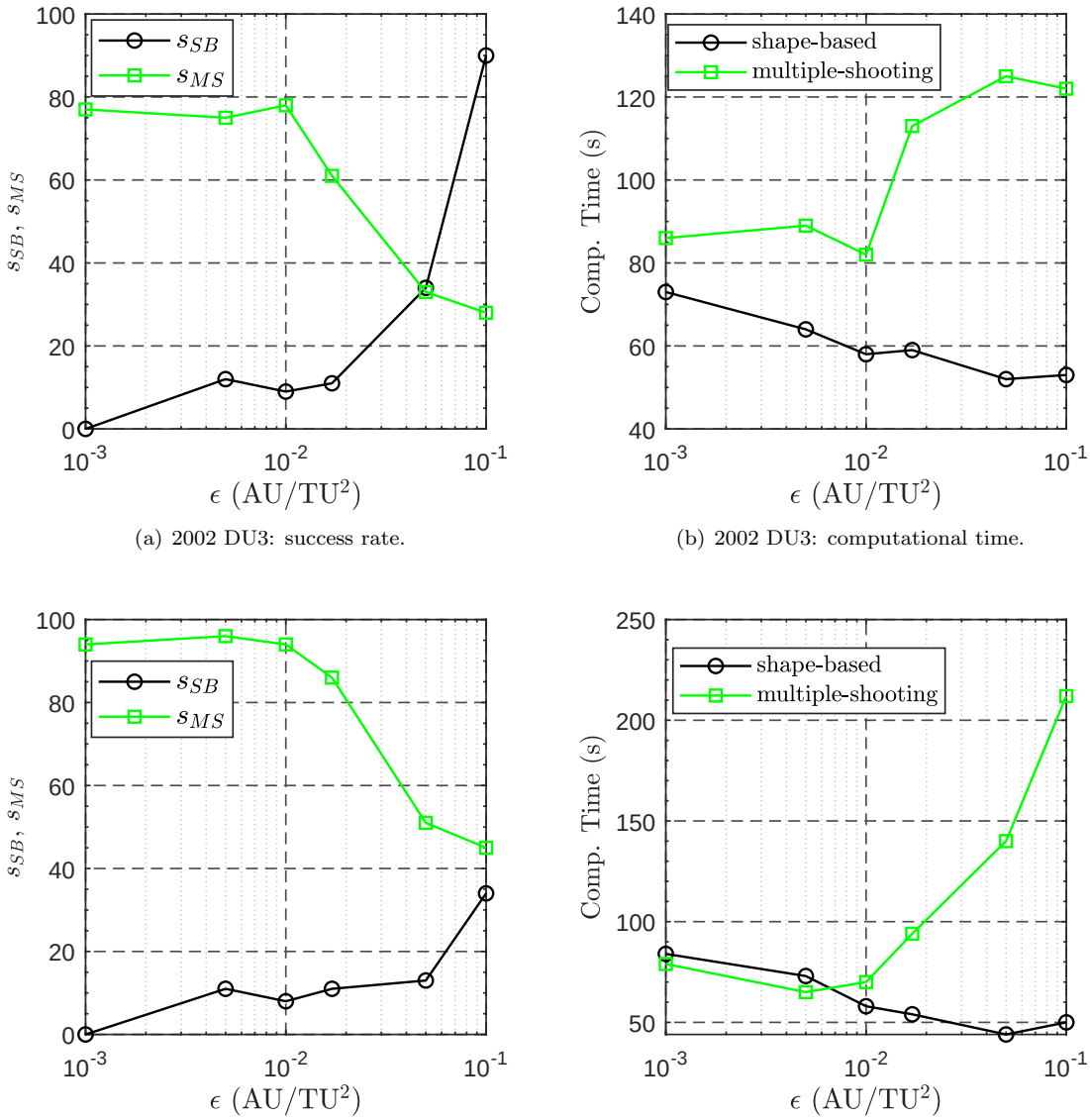

(a) 2002 DU3: success rate.

(b) 2002 DU3: computational time.

(c) 2007 MK13: success rate.

(d) 2007 MK13: computational time.

Figure 1: Success rate and mean computational time of method 1 as a function of ϵ, for an orbit-to-orbit transfer from Earth to asteroids 2002 DU3 or 2007 MK13 with $a_c = 0.3\,\mathrm{mm/s^2}$.

When a feasible solution is found, the smaller the value of ϵ, the better the approximation of the sail transfer trajectory. However, the numerical simulations have shown that finding a feasible solution for the shape-based method with very small values of ϵ is difficult (see the low success rate s_{SB} in Figs. 1(a) and 1(c)). Nevertheless, the values of ϵ for which the success rate s_{MS} is maximized are between 10^{-3} and $10^{-2}\,\mathrm{AU/TU^2}$. This is because, even if most of the solutions of the shape-based method do not satisfy the constraint equations (15)–(18), the numerical simulations have shown that these solutions are really close to be feasible and represent better approximations of solar sail trajectories than those obtained in the case

of higher values of ϵ. This can also be observed by analyzing the mean computational time required by the direct multiple-shooting approach shown in Figs. 1(b) and 1(d). Indeed, when high values of ϵ are used, the mean computational time of the direct method tends to increase, and this is probably due to the fact that the starting point provided to the nonlinear programming solver is worse than that produced with smaller values of ϵ.

The results obtained using method 2 and 3 are reported in Table 5. Both methods 2 and 3 are characterized by higher computational time and lower success rate of the direct multiple-shooting method with respect to method 1 with a low value of ϵ. In particular, the results obtained by method 2 tend to resemble those obtained by method 1 with high values of ϵ. Finally, method 3 seems unsuitable for producing good initial guesses of solar sail-based trajectories.

Target orbit	Method	s_{SB}	Comp. Time (shape-based)	s_{MS}	Comp. Time (multiple-shooting)
2002 DU3	2	93	58 s	38	104 s
2002 DU3	3	50	52 s	16	187 s
2007 MK13	2	100	45 s	46	221 s
2007 MK13	3	100	16 s	2	284 s

Table 5: Success rate and mean computational time of method 2 and 3 for an orbit-to-orbit transfer from Earth to asteroids 2002 DU3 or 2007 MK13.

The solutions obtained using the direct multiple-shooting approach are local minimum solutions, which depend on the guess generated by the shape-based approach. Therefore, for comparative purposes, the two scenarios have been also analyzed with an indirect method [8]. The minimum flight time obtained by the indirect approach is $T_{\mathrm{ind}} \simeq 14\,\mathrm{TU}$ for the transfer toward 2002 DU3, and $T_{\mathrm{ind}} \simeq 25.1\,\mathrm{TU}$ when considering a transfer to 2007 MK13. A dimensionless error Δ_{MS} (or Δ_{SB}) in the flight time between the indirect and the direct (or shape-based) method has been evaluated as

$$\Delta_{\mathrm{MS}} = \frac{T_{\mathrm{MS}} - T_{\mathrm{ind}}}{T_{\mathrm{ind}}}, \quad \Delta_{\mathrm{SB}} = \frac{T_{\mathrm{SB}} - T_{\mathrm{ind}}}{T_{\mathrm{ind}}} \tag{32}$$

where T_{MS} and T_{SB} are the minimum flight times obtained by the direct multiple-shooting and shape-based method, respectively. Figure 2 reports the values of the errors Δ_{MS} for all the solutions of the direct multiple-shooting approach and the corresponding errors Δ_{SB} of the guesses generated by the shape-based method (even those unfeasible) when $\epsilon = 10^{-2}\,\mathrm{AU/TU^2}$. The error Δ_{MS} reported in Fig. 2(b) and 2(d) is close to zero for most of the solutions, that is, the solution of the direct method is close to that found by the indirect approach. Instead, the error Δ_{SB} is larger, and in some cases the flight time can be underestimated (when Δ_{SB} takes negative values, see Fig. 2(a)). Therefore, the proposed shape-based method can provide good initial guesses for the direct multiple-shooting approach, but it may not be able to produce a good estimate of the optimal flight time in many cases.

3.1. Rendezvous scenarios

The shape-based method described above for orbit-to-orbit transfers can be easily extended to the case of ephemeris-constrained rendezvous problems. In this case, the optimization parameters are the shape parameters in Eqs. (9)–(13), the departure date t_0, the flight time T and the number of revolutions around the Sun n_{rev}. Note that the initial and final spacecraft position and velocity vectors must coincide with those of the departure and target celestial bodies, respectively. The optimization problem can be solved using the proposed shape-based procedure, in which the performance index is still the flight time T, and the constraints are given by Eqs. (15)–(18) and

$$\left| \int_{L_0}^{L_F} \frac{\mathrm{d}t}{\mathrm{d}L} \mathrm{d}L - T \right| \leq \epsilon_t \tag{33}$$

where $\mathrm{d}t/\mathrm{d}L$ can be expressed as a function of the shape functions using Eq. (24), and ϵ_t has been set equal to 2% of T in accordance with [13].

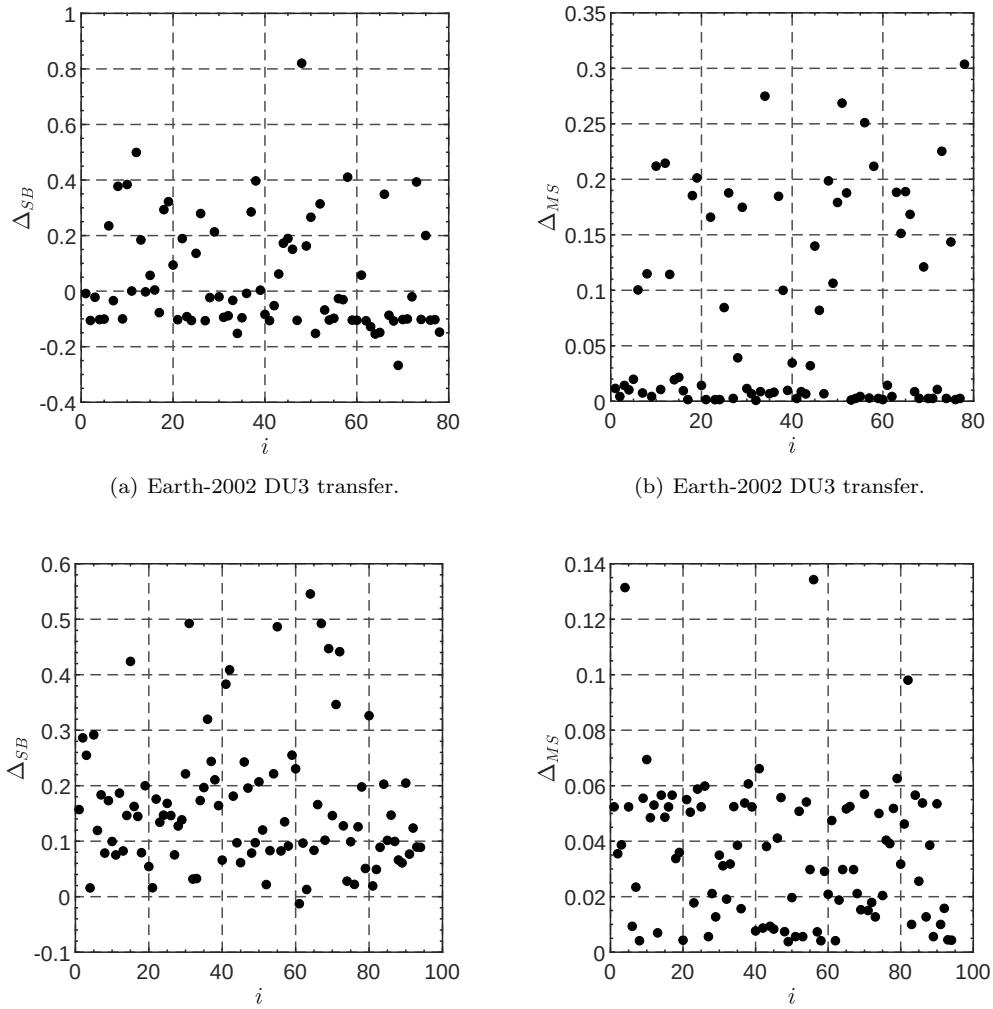

(a) Earth-2002 DU3 transfer.

(b) Earth-2002 DU3 transfer.

(c) Earth-2007 MK13 transfer.

(d) Earth-2007 MK13 transfer.

Figure 2: Error Δ_{MS} of the ith solution obtained by the direct method and error Δ_{SB} of the corresponding initial guess computed with the shape-based approach.

This procedure has been applied to rendezvous problems from Earth to the asteroids 2002 DU3 and 2007 MK13, using a solar sail with $a_c = 0.3\,\mathrm{mm/s^2}$ and a departure date between the 1st of January 2025 and 1st of January 2027. The same bounds as those reported in Table 4 are used for the shape parameters. The flight time T is constrained to assume values within the interval [5, 20] TU (or [10, 30] TU) for the transfer toward 2002 DU3 (or 2007 MK13), whereas $n_{\mathrm{rev}} \in [1, 3]$ (or $n_{\mathrm{rev}} \in [4, 7]$). As in the orbit-to-orbit case, a comparison of the three previously described methods has been performed, and the solutions of the shape-based approach have been used as initial guesses for the direct multiple-shooting approach. The results, in terms of success rates (s_{SB} and s_{MS}) and computational time, are reported in Table 6, in which the results of method 1 have been obtained using $\epsilon = 10^{-2}\,\mathrm{AU/TU^2}$.

These results show that the success rate s_{MS} of method 1 is higher than that of methods 2 and 3 also in the case of rendezvous scenarios. As a result, the best approach to solve the rendezvous problem seems to be the use of method 1 with a small value of ϵ (for example, a value $\epsilon \leq 10^{-2}\,\mathrm{AU/TU^2}$), and a direct multiple-shooting approach that uses the approximate shaped solution as its initial estimate.

Target body	Method	s_{SB}	Comp. Time (shape-based)	s_{MS}	Comp. Time (multiple-shooting)
2002 DU3	1	5	105 s	52	166 s
2002 DU3	2	58	98 s	34	164 s
2002 DU3	3	0	61 s	9	110 s
2007 MK13	1	19	105 s	51	135 s
2007 MK13	2	89	65 s	7	158 s
2007 MK13	3	0	64 s	22	183 s

Table 6: Success rate and mean computational time of method 1, 2 and 3 for Earth to 2002 DU3 and 2007 MK13 transfers.

3.2. Multiple-target missions

The shape-based method is now applied to estimate the optimal sequence of encounters in a multiple-asteroid mission starting from the Earth's orbit. In particular, three asteroids are considered as in the scenario discussed in [34]. Their orbital characteristics are reported in Table 7, and the transfer is analysed considering a solar sail with $a_c = 0.75\,\mathrm{mm/s^2}$. A simplified analysis has been carried out, in which each

celestial body	a (AU)	e	i (deg)	Ω (deg)	ω (deg)
1219 Britta	2.2130	0.1246	4.41	42.52	24.08
1831 Nicholson	2.2393	0.1277	5.63	72.60	183.48
4 Vesta	2.3614	0.0887	7.14	103.81	150.73

Table 7: Orbital parameters of asteroid 1219 Britta, 1831 Nicholson and 4 Vesta.

single trajectory leg has been computed separately assuming an orbit-to-orbit (ephemeris-free) transfer.

The optimal transfer times between any pair of celestial bodies (obtained by the shape-based method and further refined using the direct multiple-shooting approach) are reported in Table 8, whereas Table 9 shows that the most promising sequence of encounters is Earth-Britta-Nicholson-Vesta. The total computational time required to solve all the optimization problems listed in Table 8 is about 13.5 minutes. The total transfer time obtained using this simplified method is about 2010.5 days, a value lower than that reported in Ref. [34]. Of course, a second phase of mission analysis should consider the ephemeris-constrained rendezvous problem.

Scenario	T (days)
Earth-Britta	992.8
Earth-Nicholson	1019.8
Earth-Vesta	1210.6
Britta-Nicholson	497.5
Britta-Vesta	894.8
Nicholson-Britta	514.5
Nicholson-Vesta	520.1
Vesta-Britta	845.5
Vesta-Nicholson	553.9

Table 8: Optimal transfer times between any pair of celestial bodies listed in Table 7.

3.3. Comparison with other methods

This subsection presents a comparison between the proposed approach and other methods existing in the literature. The first one is the method adapted from Ref. [13] that has been already analyzed in the previous section. It has been shown how the absence of constraints modelig the solar sail propulsive acceleration leads

Scenario	T (days)
Earth-Britta-Nicholson-Vesta	2010.5
Earth-Vesta-Nicholson-Britta	2279.1
Earth-Nicholson-Vesta-Britta	2385.4
Earth-Nicholson-Britta-Vesta	2429.1
Earth-Britta-Vesta-Nicholson	2441.6
Earth-Vesta-Britta-Nicholson	2553.6

Table 9: Estimate of the total flight time required by any possible sequence of encounters.

to solutions that do not represent good estimates of solar sail-based trajectories nor good initial points for direct methods; see the results of Method 3 in Table 5.

The second approach here considered is the method proposed by Taheri and Abdelkhalik [15], which shapes the sail trajectory using finite Fourier series and takes into account the constraints equations (15)–(18). The number of Fourier series coefficients has been chosen in such a way that the total number of unknowns is equal to that of the method proposed in this work. However, the numerical simulations have shown that the genetic algorithm is unable to find any feasible solution with such an approach.

Very accurate solutions can instead be obtained using the procedure described in Ref. [16] or [17]. However, these methods are characterized by a high number of unknown variables that prevent the genetic algorithm from converging toward feasible solutions. Indeed, the techniques of Ref. [16, 17] make use of a nonlinear programming solver, and, as such, they require good starting points to find a local minimum solution. Moreover, the user is required to choose a suitable number of discretization points and Fourier series coefficients when dealing with the method of Ref. [16], or the order of the Bezier curve function for the approach of Ref. [17], which may depend on the particular mission scenario. This implies a higher user-computer interaction with respect to the proposed method. The strength of the approach here discussed, instead, is that it can automate the whole optimization procedure, and, therefore, it is especially advisable when a large number of mission cases must be investigated.

Other methods exist to obtain fast estimates of the flight time between two arbitrary orbits, such as that proposed in [6], based on the use of deep neural networks. However, unlike the method proposed in this paper, such an approach does not provide the solar sail optimal transfer trajectory nor the optimal control law. Moreover, the method of Ref. [6] has been applied only to scenarios that consider a solar sail with characteristic acceleration of $0.75\,\mathrm{mm/s^2}$. Finally, other approaches based on the use of homotopy methods can find very accurate solutions. An example is given in Ref. [35], which, anyway, requires an initialization with the solution of a low-thrust transfer problem. In other terms, an initial guess of costates of the low-thrust transfer solution is required to start the homotopy method, although their estimate in a large number of flight scenarios may be a difficult and time-consuming task. Moreover, Ref. [35] only considers simple coplanar circle-to-circle transfers or rendezvous toward celestial bodies with moderate values of orbital inclination and eccentricity, whereas the shape-based approach here proposed is able to deal with more involved cases without requiring any initializing solution.

4. Conclusions

This work presented a shape-based method able to generate approximate optimal solar sail-based trajectories for heliocentric transfer scenarios. Novel shape functions have been introduced that describe the evolution of modified equinoctial elements for three-dimensional transfers, whose analytical expressions have been chosen by analyzing actual (optimal) transfer trajectories. An optimization problem has been formulated, which consists in computing a set of shaping coefficients to obtain a minimum-time orbit transfer. Also, a set of nonlinear constraint equations has been enforced on the propulsive acceleration vector in order to get solutions that are as close as possible to feasible solar sail-based trajectories.

The proposed method has been validated using three-dimensional orbit-to-orbit and rendezvous transfer scenarios. Extensive numerical simulations have shown that although the shape-based method is not always able to give an accurate estimate of the optimal (minimum) transfer time, the solutions it finds out are still better approximations of solar sail trajectories than those obtained using other shape-based methods existing

in the literature, which usually provide general low-thrust trajectories that do not satisfy the classical solar sail (physical) limitations. Finally, the proposed approach is also usually effective in providing good initial guesses for direct methods.

Conflict of interest statement

The authors declared that they have no conflicts of interest to this work.

References

[1] S. Gong, M. Macdonald, Review on solar sail technology, Astrodynamics 3 (2) (2019) 93–125, doi: 10.1007/s42064-019-0038-x.

[2] X. Pan, M. Xu, R. Santos, Trajectory optimization for solar sail in cislunar navigation constellation with minimal lightness number, Aerospace Science and Technology 70 (2017) 559–567, doi: 10.1016/j.ast.2017.08.042.

[3] L. Niccolai, G. Mengali, A. A. Quarta, A. Caruso, Feedback control law of solar sail with variable surface reflectivity at sun-earth collinear equilibrium points, Aerospace Science and Technology, Article number 106144. 106, doi: 10.1016/j.ast.2020.106144.

[4] S. Gong, J. Li, Spin-stabilized solar sail for displaced solar orbits, Aerospace Science and Technology 32 (1) (2014) 188–199, doi: 10.1016/j.ast.2013.10.002.

[5] A. Peloni, M. Ceriotti, B. Dachwald, Solar-sail trajectory design for a multiple near-earth-asteroid rendezvous mission, Journal of Guidance, Control, and Dynamics 39 (12) (2016) 2712–2724, doi: 10.2514/1.G000470.

[6] Y. Song, S. Gong, Solar-sail trajectory design for multiple near-earth asteroid exploration based on deep neural networks, Aerospace Science and Technology 91 (2019) 28–40, doi: 10.1016/j.ast.2019.04.056.

[7] J. T. Betts, Survey of numerical methods for trajectory optimization, Journal of Guidance, Control, and Dynamics 21 (2) (1998) 193–207, doi: 10.2514/2.4231.

[8] G. Mengali, A. A. Quarta, Rapid solar sail rendezvous missions to asteroid 99942 Apophis, Journal of Spacecraft and Rockets 46 (1) (2009) 134–140, doi: 10.2514/1.37141.

[9] C. G. Sauer, Optimum solar-sail interplanetary trajectories, in: AIAA/AAS Astrodynamics Conference, San Diego (CA), 1976.

[10] L. Niccolai, A. A. Quarta, G. Mengali, Analytical solution of the optimal steering law for non-ideal solar sail, Aerospace Science and Technology 62 (2017) 11–18, doi: 10.1016/j.ast.2016.11.031.

[11] A. Farrés, J. Heiligers, N. Miguel, Road map to L4/L5 with a solar sail, Aerospace Science and Technology, Article number 105458. 95, doi: 10.1016/j.ast.2019.105458.

[12] A. E. Petropoulos, J. M. Longuski, Shape-based algorithm for automated design of low-thrust, gravity-assist trajectories, Journal of Spacecraft and Rockets 41 (5) (2004) 787–796, doi: 10.2514/1.13095.

[13] P. De Pascale, M. Vasile, Preliminary design of low-thrust multiple gravity-assist trajectories, Journal of Spacecraft and Rockets 43 (5) (2006) 1065–1076, doi: 10.2514/1.19646.

[14] B. J. Wall, B. A. Conway, Shape-based approach to low-thrust rendezvous trajectory design, Journal of Guidance, Control, and Dynamics 32 (1) (2009) 95–102, doi: 10.2514/1.36848.

[15] E. Taheri, O. Abdelkhalik, Initial three-dimensional low-thrust trajectory design, Advances in Space Research 57 (3) (2016) 889–903, doi: 10.1016/j.asr.2015.11.034.

[16] A. Caruso, M. Bassetto, G. Mengali, A. A. Quarta, Optimal solar sail trajectory approximation with finite fourier series, In press. Advances in Space Research doi: 10.1016/j.asr.2019.11.019.

[17] M. Huo, Z. Yu, H. Liu, C. Zhao, T. Lin, Z. Song, N. Qi, Initial three-dimensional trajectory design for solar sails using bezier shaping approach, IEEE Access Article number 8871191. 7 (2019) 150842–150850, doi: 10.1109/ACCESS.2019.2947721.

[18] M. Huo, G. Mengali, A. A. Quarta, N. Qi, Electric sail trajectory design with bezier curve-based shaping approach, Aerospace Science and Technology 88 (2019) 126–135, doi: 10.1016/j.ast.2019.03.023.

[19] A. Peloni, A. V. Rao, M. Ceriotti, Automated trajectory optimizer for solar sailing (atoss), Aerospace Science and Technology 72 (2018) 465–475, doi: 10.1016/j.ast.2017.11.025.

[20] B. Dachwald, G. Mengali, A. A. Quarta, M. Macdonald, Parametric model and optimal control of solar sails with optical degradation, Journal of Guidance, Control, and Dynamics 29 (5) (2006) 1170–1178, doi: 10.2514/1.20313.

[21] C. R. McInnes, Solar Sailing: Technology, Dynamics and Mission Applications, Springer-Verlag Berlin, 1999, Ch. 2, pp. 46–51, ISBN: 978-1-85233-102-3.

[22] A. Caruso, G. Mengali, A. A. Quarta, L. Niccolai, Solar sail optimal control with solar irradiance fluctuations, In press. Advances in Space Research doi: 10.1016/j.asr.2020.05.037.

[23] M. J. H. Walker, B. Ireland, J. Owens, A set modified equinoctial orbit elements, Celestial Mechanics 36 (4) (1985) 409–419, doi: 10.1007/BF01227493.

[24] M. J. Walker, Erratum - a set of modified equinoctial orbit elements, Celestial Mechanics 38 (1986) 391–392, doi: 10.1007/BF01238929.

[25] A. E. Bryson, Y. C. Ho, Applied Optimal Control, Hemisphere Publishing Corporation, New York, 1975, Ch. 2, pp. 71–89, ISBN: 0-891-16228-3.

[26] A. R. Conn, N. I. Gould, P. L. Toint, Globally convergent augmented lagrangian algorithm for optimization with general constraints and simple bounds, SIAM Journal on Numerical Analysis 28 (2) (1991) 545–572, doi: 10.1137/0728030.

[27] A. Conn, N. Gould, P. Toint, A globally convergent lagrangian barrier algorithm for optimization with general inequality constraints and simple bounds, Mathematics of Computation 66 (217) (1997) 261–288, doi: 10.1090/S0025-5718-97-00777-1.

[28] R. Lewis, V. Torczon, A globally convergent augmented lagrangian pattern search algorithm for optimization with general constraints and simple bounds, SIAM Journal on Optimization 12 (4) (2002) 1075–1089, doi: 10.1137/S1052623498339727.
[29] M. Li, Y. Huang, S. Gong, Assessing the risk of potentially hazardous asteroids through mean motion resonances analyses, Astrophysics and Space Science Article number 78. 364 (5), doi: 10.1007/s10509-019-3557-5.
[30] A. Thirouin, N. A. Moskovitz, R. P. e. a. Binzel, The mission accessible near-earth objects survey: Four years of photometry, Astrophysical Journal, Supplement Series Article number 4. 239 (1), doi: 10.3847/1538-4365/aae1b0.
[31] M. Hicks, J. Somers, 2007 mk13: A highly elongated c-type potentially hazardous asteroid, The Astronomer's Telegram 2372 (2010) 1 .
[32] J. A. E. Andersson, J. Gillis, G. Horn, J. B. Rawlings, M. Diehl, CasADi: a software framework for nonlinear optimization and optimal control, Mathematical Programming Computation 11 (1), doi: 10.1007/s12532-018-0139-4.
[33] A. Wächter, L. T. Biegler, On the implementation of an interior-point filter line-search algorithm for large-scale nonlinear programming, Mathematical Programming 106 (1) (2006) 25–57, doi: 10.1007/s10107-004-0559-y.
[34] Y. Song, S. Gong, Solar sail trajectory optimization of multi-asteroid rendezvous mission, Acta Astronautica 157 (2019) 111–122, doi: 10.1016/j.actaastro.2018.12.016.
[35] N. Sullo, A. Peloni, M. Ceriotti, Low-thrust to solar-sail trajectories: A homotopic approach, Journal of Guidance, Control, and Dynamics 40 (11) (2017) 2796–2806, doi: 10.2514/1.G002552.

View publication stats